A mechanical metamaterial made from a DNA hydrogel

Jong Bum Lee[1,2][†], Songming Peng[1][†], Dayong Yang[1], Young Hoon Roh[1], Hisakage Funabashi[1,3], Nokyoung Park[1,4], Edward J. Rice[1], Liwei Chen[5], Rong Long[1], Mingming Wu[1] and Dan Luo[1]★

Metamaterials are artificial substances that are structurally engineered to have properties not typically found in nature. To date, almost all metamaterials have been made from inorganic materials such as silicon and copper[1,2], which have unusual electromagnetic or acoustic properties[1-5] that allow them to be used, for example, as invisible cloaks[6-9], superlenses[10-12] or super absorbers for sound[13]. Here, we show that metamaterials with unusual mechanical properties can be prepared using DNA as a building block. We used a polymerase enzyme to elongate DNA chains and weave them noncovalently into a hydrogel. The resulting material, which we term a meta-hydrogel, has liquid-like properties when taken out of water and solid-like properties when in water. Moreover, upon the addition of water, and after complete deformation, the hydrogel can be made to return to its original shape. The meta-hydrogel has a hierarchical internal structure and, as an example of its potential applications, we use it to create an electric circuit that uses water as a switch.

We have previously developed bulk-scale, DNA-based materials[14-20] that can be used in practical applications such as multiplexed diagnosis[17,19,21], vaccine and drug delivery[22-24] and cell-free protein production[20]. In particular, we created a hydrogel that was made entirely of DNA and crosslinked by enzymes (T4 ligase)[18]. In the present work we take a different approach. Instead of crosslinking DNA chains covalently into a chemical hydrogel (via a ligase), we have elongated DNA chains and woven them noncovalently into a physical hydrogel (via a polymerase). To fabricate our DNA meta-hydrogel, we chose a special polymerase, Φ29, a bacteria phage polymerase that is capable of DNA chain elongation and displacement, thus amplifying and weaving DNA[25]. Φ29 uses a single-stranded DNA (ssDNA) as a template to elongate the primer, while at the same time displacing the newly synthesized strands into ssDNA products. Based on Φ29, we designed a unique combination of two sequential processes: (i) a rolling circle amplification (RCA, or **R**) followed by (ii) a multi-primed chain amplification (MCA, or **M**). After running the RCA for x hours followed by the MCA for y hours, a chain reaction was established, resulting in a DNA hydrogel (Fig. 1, Supplementary Fig. S1, Table S1 and Discussion SI). To simplify the notation, we abbreviate our procedures as $R_x M_y$.

The enzymatic processes were monitored by observing the optical density (OD_{600}). For example, when the **R**-process was set at 4 h, the OD increased with the duration of the **M**-process (Supplementary Fig. S2). When the **M**-process reached 16 h ($R_4 M_{16}$), a totally opaque gel was obtained (Fig. 2a). As expected, this hydrogel showed fluorescence after staining with a DNA-specific dye (GelGreen, Fig. 2b), indicating that the entire hydrogel

was composed of DNA. Rheology data further confirmed that the $R_4 M_{16}$ was a true gel, as the shear-storage modulus (G') was constantly higher than the shear-loss modulus (G'') over the entire frequency range (Fig. 2c). On the other hand, when the **R**-process continued alone for 20 h ($R_{20} M_0$), a viscous solution was produced (Supplementary Fig. S2), and there were no detectable signals in the rheometer, proving that the $R_{20} M_0$ was just a liquid. We further tested the gel formation by varying the combinations of x and y and found that a minimum of $x = 2$ h and $y = 16$ h was required to create a DNA hydrogel (Supplementary Table S2). As expected[26], the hydrogel in solution melted at 85 °C due to denaturing of the DNA strands (Supplementary Fig. S3).

Unexpectedly, we discovered unusual metaproperties in our DNA hydrogel—it had either liquid-like or solid-like properties depending on the physical environment. When the gel was taken out of water it became a 'liquid' that flowed freely in a tube (Fig. 3a), and when placed in differently shaped containers conformed to the shape of the containers (Fig. 3b). However, when put back into water, it metamorphosed into a solid gel. We emphasize that although the hydrogel behaved like a liquid, it was still a gel. Surprisingly, it always returned rapidly to its original shape in water, regardless of how many different shapes it had adopted while in the liquid-like state. To further investigate this unusual property, we first formed $R_4 M_{16}$ meta-hydrogel in moulds with defined geometries in the shape of the letters D, N and A (Fig. 3c). After removing water, each hydrogel behaved like a liquid by conforming to the shape of the vial (Fig. 3d). However, when the water was reintroduced, the hydrogels returned to their original shapes (D, N and A) within 15 s (Fig. 3e–f). The entire event was captured by video (Supplementary Movie S1). These liquid–solid transition and returning-to-original-shape processes can be repeated as many times as required. Furthermore, the hydrogel can be remoulded into new shapes upon heating the gel above its denaturing temperature (Supplementary Fig. S4). These results therefore clearly demonstrate the fabrication of a novel organic-based metamaterial.

Unlike conventional hydrogels, which have amorphous internal structures[18,20,27], our $R_4 M_{16}$ meta-hydrogel has a hierarchical internal structure, as revealed by field-emission scanning electron microscopy (FESEM). At the microscale, the densely packed DNA microstructures are in the shape of a bird nest (Fig. 4a,b). These nest structures are of uniform size and woven together by DNA. Within each microstructure, the internal porous nanostructures were observed by cutting the DNA nest in half using a focused ion beam (Fig. 4c). To the best of our knowledge, this hierarchical structural organization has not previously been seen in hydrogels, and may contribute to its metaproperties.

[1]Department of Biological and Environmental Engineering, Cornell University, Ithaca, New York 14853, USA, [2]Department of Chemical Engineering, University of Seoul, Seoul 130-743, South Korea, [3]Institute for Sustainable Sciences and Development, Hiroshima University, Higashi-Hiroshima City 739-8511, Japan, [4]Frontier Research Lab., Samsung Advanced Institute of Technology 449-712, South Korea, [5]Suzhou Institute of Nano-Tech and Nano-Bionics, Chinese Academy of Sciences, Suzhou 215123, China; [†]These authors contributed equally to this work. *e-mail: dan.luo@cornell.edu
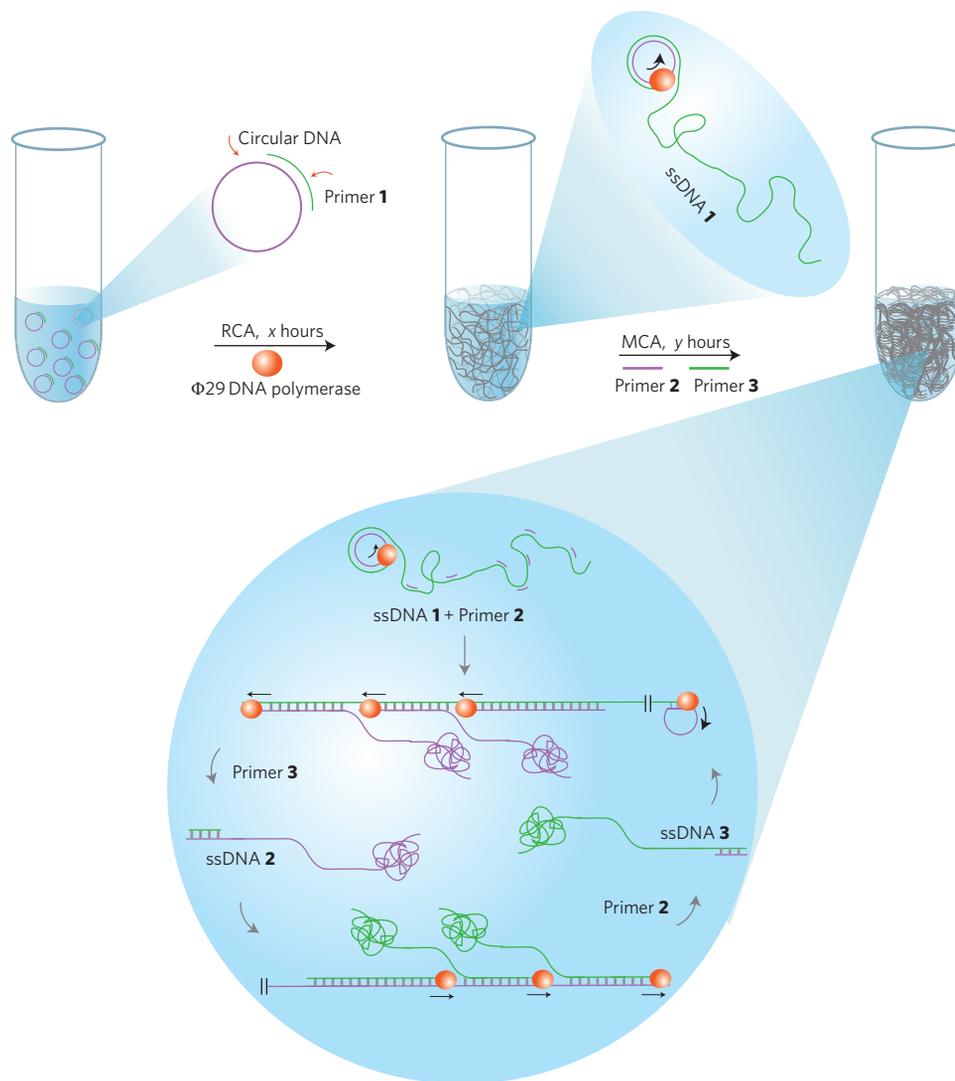
Figure 1 | Schematic diagram of the stepwise approach for DNA hydrogel synthesis. The RCA and MCA processes were carried out as follows. (i) In the **R** process, a circular ssDNA template was first produced (Supplementary Fig. S1 and Table S1), then a complementary primer for RCA (Primer 1) was added to produce elongated ssDNA products (termed ssDNA 1: tandem repeats of the sequences complementary to the original circular ssDNA template). (ii) In the **M** process, after RCA, we added two additional primers (Primer 2 and Primer 3) for subsequent chain amplification. Primer 2 was elongated to generate ssDNA 2 (complementary to ssDNA-1). Primer 3 was used to create ssDNA 3 (complementary to ssDNA 2; thus ssDNA 3 and ssDNA 1 had exactly the same sequences). Primer 2 was also therefore able to produce more ssDNA 2 using newly synthesized ssDNA 3 as templates, leading to chain amplification.
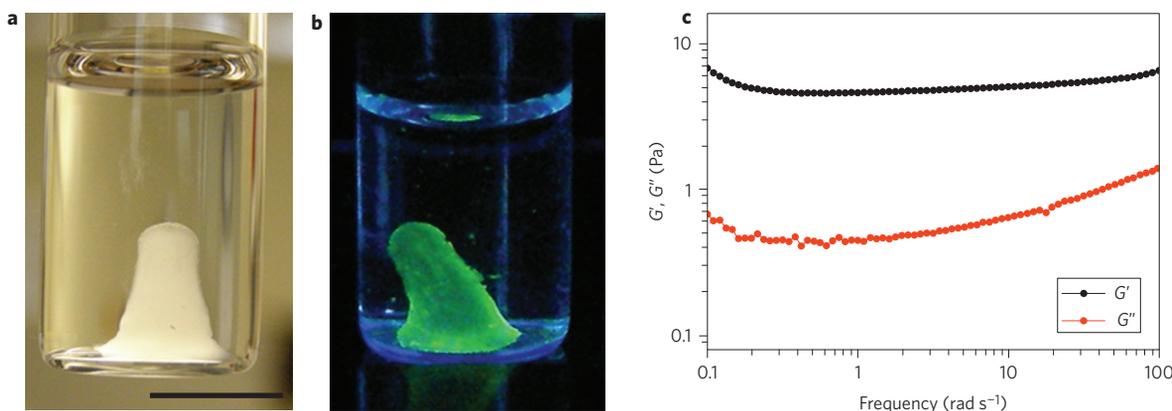
Figure 2 | Characterization of the R_4M_{16} DNA hydrogel. a, Photograph of the R_4M_{16} hydrogel. Scale bar, 10 mm. **b**, Hydrogels stained with GelGreen, a DNA-specific dye. **c**, Storage-loss (G') and shear-loss (G'') moduli of R_4M_{16} hydrogel from a rheometer measurement.
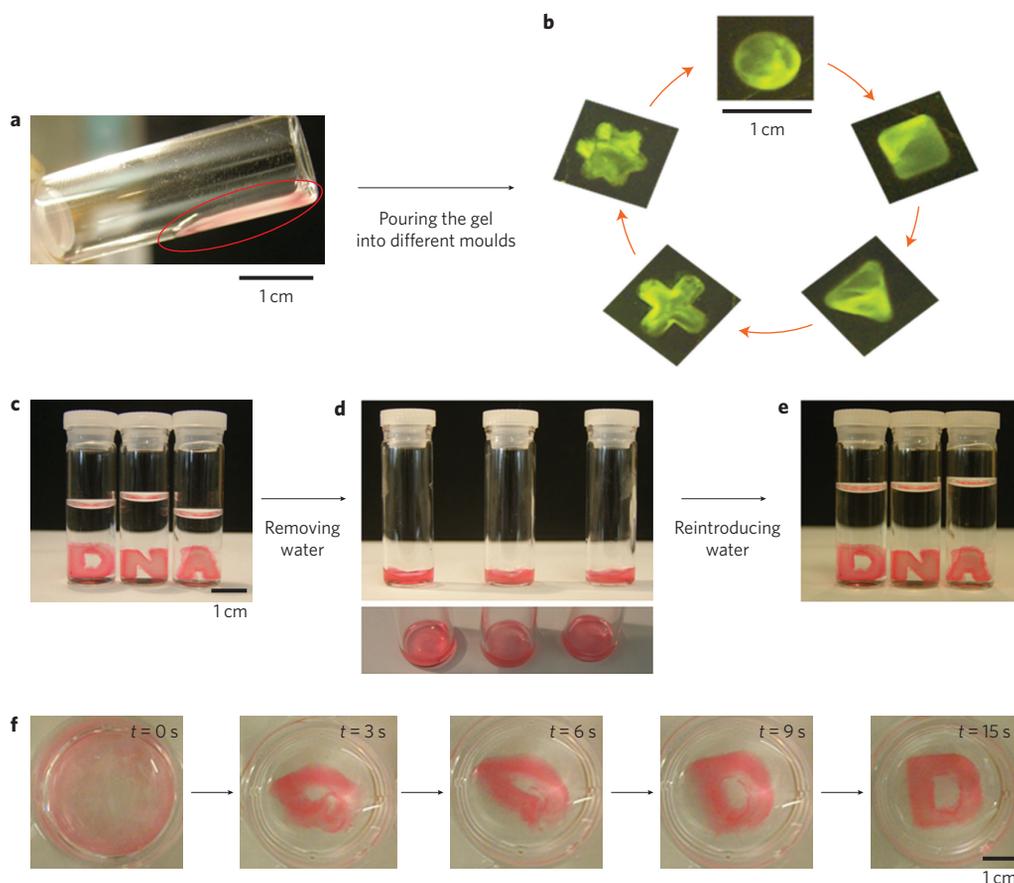
Figure 3 | Liquid- and solid-like properties of the R_4M_{16} hydrogel. a, When out of water, the hydrogel flows freely in the tube. **b**, When poured into differently shaped containers consecutively and repeatedly (from circular, to square, to triangular, to X-shaped, to star-shaped, then back to circular), the hydrogel conforms to the shape of the container, just like a liquid. The gel was stained with GelGreen. **c**, D-, N- and A-shaped hydrogel was successfully formed and its solid-like property tested by removing and replacing water. **d–f**, Series of photographs showing the process of DNA hydrogel returning to its original shape after reintroducing water at 25 °C: the gels begin to metamorphose within the first 3 s ($t = 0$–3 s). The gel continues to transform back to its original shape, gradually and smoothly ($t = 3$–9 s). The final D shape is restored within 15 s ($t = 15$ s).

We further selectively tuned the hierarchical microstructures by separately changing the reaction times of **R** and **M**. More specifically, by increasing the **M** reaction time from 1 h to 16 h while keeping **R** constant at 4 h (that is, R_4M_1, R_4M_3, R_4M_6 and R_4M_{16}), we produced more developed DNA bird nests (Supplementary Fig. S5a–d). The diameter of the bird nest increased from ∼0.3 μm in R_4M_1 to ∼1.6 μm in R_4M_{16}. On the other hand, by lengthening the **R** process from 0 h to 8 h while keeping **M** constant at 16 h (that is, R_0M_{16}, R_1M_{16}, R_2M_{16}, R_4M_{16} and R_8M_{16}), we obtained more densely populated bird nests of almost identical size (Fig. 4d–h, the number of bird nests were from $10 \pm 2/100$ μm^2 in R_0M_{16} to $35 \pm 5/100$ μm^2 in R_8M_{16}). We emphasize that these differently tuned hierarchical internal structures (in terms of size and density of the DNA bird nests) were accomplished by designing and controlling the enzymatic reactions of R_xM_y.

Through the morphology studies we discovered that the two enzymatic reactions **R** and **M** determine the internal hierarchical structures, which in turn leads to the observed metaproperties. Indeed, the metaproperties are only found when $x = 2$–8 h and $y \geq 16$ h (Supplementary Table S2). Although the complete mechanism for the metaproperties is still subject to investigation, we propose the following theory. From an enzymatic perspective and based on the well-known characteristics of Φ29 and the design of our unique primers, the **R** process first generates a large number of long tandem ssDNA, which in turn serve as templates for the **M** process, the products of which are both long ssDNA and

dsDNA. As revealed in the morphology studies, these DNA strands are woven together into bird nests as well as linear bundles by enzymatic processes. From a physics aspect, we attribute the liquid- and solid-like properties to the ultralow elastic modulus of our DNA hydrogel. When a hydrogel is exposed to air, the gel is deformed by surface tension and gravity, which is energetically penalized by the strain energy due to elastic deformation. Such deformation due to surface tension and gravity is negligible for most solids as the strain energy penalty is too high because of the large modulus E (ranging from kPa to GPa)[18,28,29]. However, because our DNA hydrogel is extremely soft ($E \approx 10$ Pa; Fig. 2c, Supplementary Fig. S6), both the surface energy and the gravitational energy completely outweigh the strain energy. As a result, the gel shape is primarily determined by surface tension and gravity when exposed to air and it behaves like a liquid. When the gel is immersed in water, on the other hand, the surface tension is practically zero, and buoyancy forces cancel the gravity. Thus, the hydrogel behaves like a solid and retains its original shape. The whole process is illustrated in Supplementary Fig. S7, and more theoretical calculations are deduced in Supplementary Discussion SII.

A variety of applications can be envisioned using either or both liquid-like and solid-like properties of our meta-gels. As an example, we designed a DNA-meta-hydrogel-based electric circuit that uses water as a switch (Fig. 5). When the surrounding water was removed, the DNA meta-hydrogel (doped with 10 nm gold
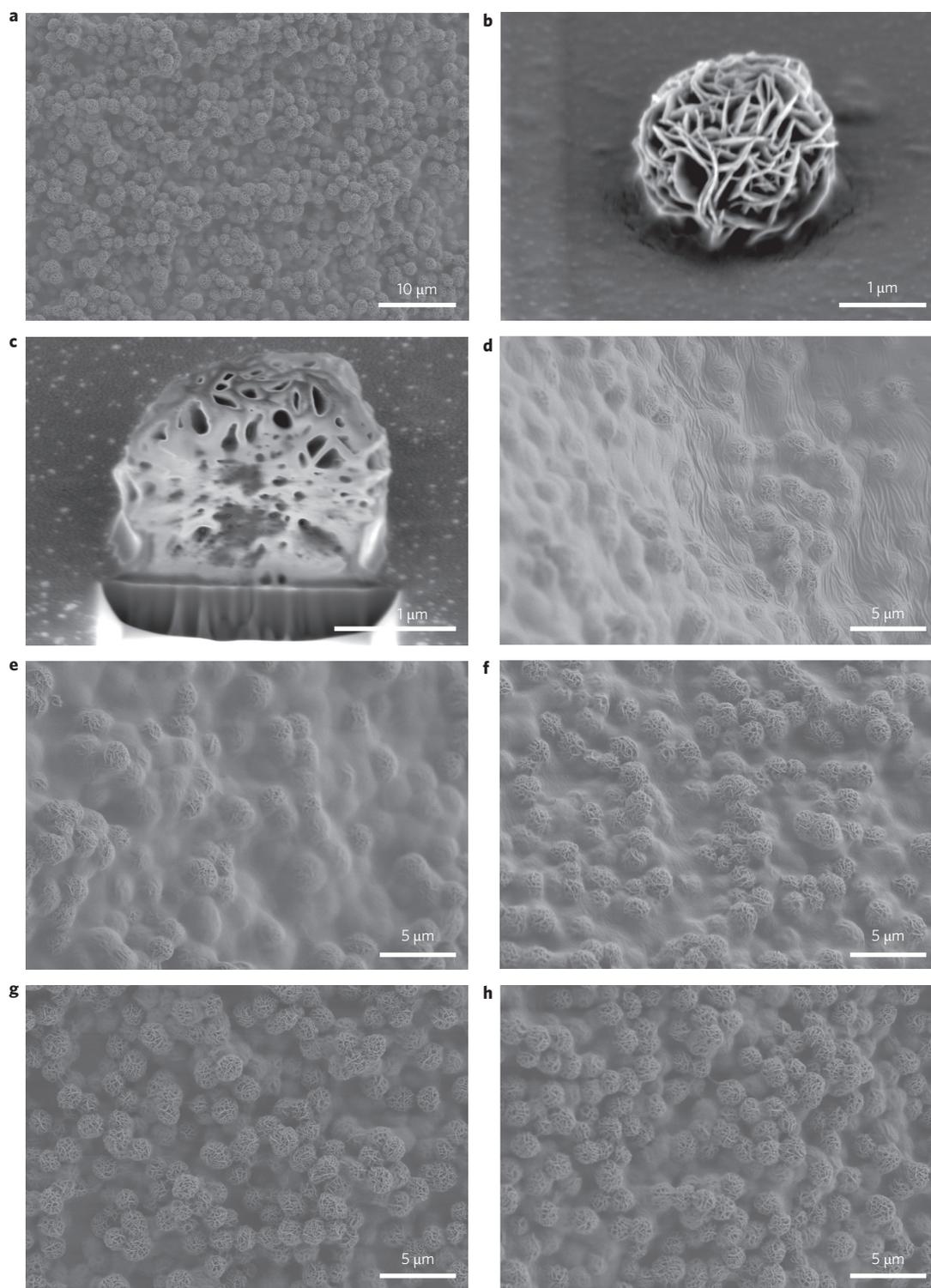
Figure 4 | Morphology of the DNA hydrogel. a, SEM images of R_4M_{16} DNA hydrogel. **b,c**, SEM images of an individual DNA bird nest, which was isolated (**b**) then cut with a focused ion beam (**c**). **d–h**, SEM images for different RCA times: R_0M_{16} (**d**), R_1M_{16} (**e**), R_2M_{16} (**f**), R_4M_{16} (**g**) and R_8M_{16} (**h**).

nanoparticles to provide electric conductivity) became 'liquid-like' and thus conformed to the shape of the channel linking the two electrodes together. As a result, the circuit was turned on (Fig. 5, 'ON'). By simply adding water to the meta-hydrogel, it once again became 'solid-like' and returned to its original, shorter shape, thereby causing the gel to rapidly move away from the electrode and completely shut off the current (Fig. 5, 'OFF'). This simple demonstration shows one application that takes advantage of the

metaproperties of our meta-hydrogel, but it can also be applied to biomedical applications such as controlled drug release for multiple drugs (Supplementary Fig. S8). More applications in other fields are also being explored.

In conclusion, we have designed and programmed two enzyme processes to achieve a novel DNA meta-hydrogel. These specifically designed enzymatic processes generate a striking internal morphology with hierarchical structure and confer our DNA hydrogel
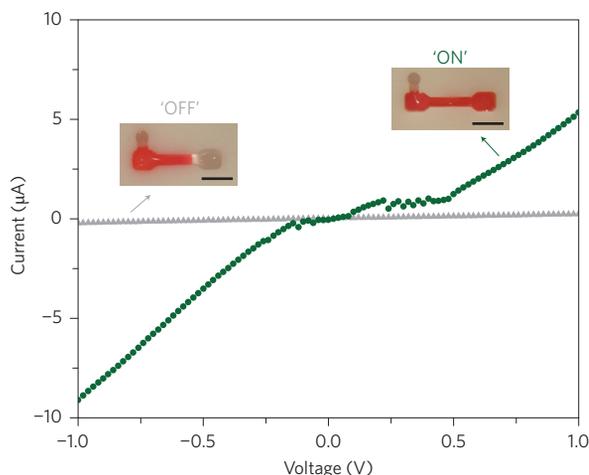
Figure 5 | Electric circuit switch formed using the liquid- and solid-like properties of DNA meta-hydrogel. When the DNA meta-hydrogel (containing 10 nm gold nanoparticles) has liquid-like properties, the circuit can be covered by the gel (green circles, 'ON'). By simply adding water, the gel metamorphoses to its original shape, which is shorter, resulting in the gel rapidly moving away (within seconds) from the electrode and completely shutting off the current (grey triangles, 'OFF'). Scale bars (insets), 5 mm.

with metaproperties. The DNA meta-hydrogel notably expands the metamaterial repertoire and has potential for real-world applications, including drug release, cell therapy, electric switches and flexible circuits.

References

1. Shelby, R. A., Smith, D. R. & Schultz, S. Experimental verification of a negative index of refraction. *Science* **292,** 77–79 (2001).
2. Liu, Y. M. & Zhang, X. Metamaterials: a new frontier of science and technology. *Chem. Soc. Rev.* **40,** 2494–2507 (2011).
3. Pendry, J. B., Holden, A. J., Stewart, W. J. & Youngs, I. Extremely low frequency plasmons in metallic mesostructures. *Phys. Rev. Lett.* **76,** 4773–4776 (1996).
4. Smith, D. R., Padilla, W. J., Vier, D. C., Nemat-Nasser, S. C. & Schultz, S. Composite medium with simultaneously negative permeability and permittivity. *Phys. Rev. Lett.* **84,** 4184–4187 (2000).
5. Smith, D. R., Pendry, J. B. & Wiltshire, M. C. K. Metamaterials and negative refractive index. *Science* **305,** 788–792 (2004).
6. Alu, A. & Engheta, N. Achieving transparency with plasmonic and metamaterial coatings. *Phys. Rev. E* **72,** 016623 (2005).
7. Schurig, D. *et al.* Metamaterial electromagnetic cloak at microwave frequencies. *Science* **314,** 977–980 (2006).
8. Liu, R. *et al.* Broadband ground-plane cloak. *Science* **323,** 366–369 (2009).
9. Fridman, M., Farsi, A., Okawachi, Y. & Gaeta, A. L. Demonstration of temporal cloaking. *Nature* **481,** 62–65 (2012).
10. Grbic, A. & Eleftheriades, G. V. Overcoming the diffraction limit with a planar left-handed transmission-line lens. *Phys. Rev. Lett.* **92,** 117403 (2004).
11. Fang, N., Lee, H., Sun, C. & Zhang, X. Sub-diffraction-limited optical imaging with a silver superlens. *Science* **308,** 534–537 (2005).
12. Rogers, E. T. F. *et al.* A super-oscillatory lens optical microscope for subwavelength imaging. *Nature Mater.* **11,** 432–435 (2012).
13. Mei, J. *et al.* Dark acoustic metamaterials as super absorbers for low-frequency sound. *Nature Commun.* **3,** 756 (2012).
14. Roh, Y. H., Ruiz, R. C. H., Peng, S. M., Lee, J. B. & Luo, D. Engineering DNA-based functional materials. *Chem. Soc. Rev.* **40,** 5730–5744 (2011).
15. Tan, S. J., Campolongo, M. J., Luo, D. & Cheng, W. L. Building plasmonic nanostructures with DNA. *Nature Nanotech.* **6,** 268–276 (2011).
16. Li, Y. G. *et al.* Controlled assembly of dendrimer-like DNA. *Nature Mater.* **3,** 38–42 (2004).
17. Li, Y. G., Cu, Y. T. H. & Luo, D. Multiplexed detection of pathogen DNA with DNA-based fluorescence nanobarcodes. *Nature Biotechnol.* **23,** 885–889 (2005).
18. Um, S. H. *et al.* Enzyme-catalysed assembly of DNA hydrogel. *Nature Mater.* **5,** 797–801 (2006).
19. Lee, J. B. *et al.* Multifunctional nanoarchitectures from DNA-based ABC monomers. *Nature Nanotech.* **4,** 430–436 (2009).
20. Park, N., Um, S. H., Funabashi, H., Xu, J. F. & Luo, D. A cell-free protein-producing gel. *Nature Mater.* **8,** 432–437 (2009).
21. Feng, X. L. *et al.* Fluorescence logic-signal-based multiplex detection of nucleases with the assembly of a cationic conjugated polymer and branched DNA. *Angew. Chem. Int. Ed.* **48,** 5316–5321 (2009).
22. Sil, D., Lee, J. B., Luo, D., Holowka, D. & Baird, B. Trivalent ligands with rigid DNA spacers reveal structural requirements for IgE receptor signaling in RBL mast cells. *ACS Chem. Biol.* **2,** 674–684 (2007).
23. Cheng, E. J. *et al.* A pH-triggered, fast-responding DNA hydrogel. *Angew. Chem. Int. Ed.* **48,** 7660–7663 (2009).
24. Rattanakiat, S., Nishikawa, M., Funabashi, H., Luo, D. & Takakura, Y. The assembly of a short linear natural cytosine–phosphate–guanine DNA into dendritic structures and its effect on immunostimulatory activity. *Biomaterials* **30,** 5701–5706 (2009).
25. Dean, F. B., Nelson, J. R., Giesler, T. L. & Lasken, R. S. Rapid amplification of plasmid and phage DNA using phi29 DNA polymerase and multiply-primed rolling circle amplification. *Genome Res.* **11,** 1095–1099 (2001).
26. Lee, J. B., Shai, A. S., Campolongo, M. J., Park, N. & Luo, D. Three-dimensional structure and thermal stability studies of DNA nanostructures by energy transfer spectroscopy. *ChemPhysChem* **11,** 2081–2084 (2010).
27. Roh, Y. H. *et al.* Photocrosslinked DNA nanospheres for drug delivery. *Macromol. Rapid Commun.* **31,** 1207–1211 (2010).
28. Cauich-Rodriguez, J. V., Deb, S. & Smith, R. Effect of cross-linking agents on the dynamic mechanical properties of hydrogel blends of poly(acrylic acid)–poly(vinyl alcohol vinyl acetate). *Biomaterials* **17,** 2259–2264 (1996).
29. Xing, Y. Z. *et al.* Self-assembled DNA hydrogels with designable thermal and enzymatic responsiveness. *Adv. Mater.* **23,** 1117–1121 (2011).

Author contributions

J.B.L., S.P. and D.L. designed the experiments. J.B.L., S.P., Y.H.R., H.F., N.P. and E.R. carried out the experiments. J.B.L., S.P., Y.H.R., H.F., D.Y., L.C., R.L., M.W. and D.L. contributed to the data analysis. J.B.L., S.P., Y.H.R., D.Y., R.L. and D.L. wrote the manuscript.

Additional information

Supplementary information is available in the online version of the paper. Reprints and permission information is available online at http://www.nature.com/reprints. Correspondence and requests for materials should be addressed to D.L.

Competing financial interests

The authors declare no competing financial interests.

3 ## A mechanical metamaterial made from DNA hydrogel

4 Jong Bum Lee*, Songming Peng*, Dayong Yang, Young Hoon Roh, Hisakage Funabashi,

5 Nokyoung Park, Edward J Rice, Liwei Chen, Rong Long, Mingming Wu, Dan Luo**

6

7 ## Materials and Methods

8 ### Chemicals and DNA sequences

9 Φ29 DNA polymerase was purchased from New England Biolabs (Beverly, MA)

10 in pure form at a concentration of 10,000 units/ml. Oligonucleotides were commercially

11 synthesized and PAGE purified (Integrated DNA Technologies, Coralville, Iowa).

12 Sequences of the oligonucleotides are listed in Table S1.

13 ### Preparation of circular DNA templates

14 0.5 µM of phosphorylated linear ssDNA was treated with 5 unit/µl of CircLigase

15 ssDNA Ligase (Epicentre Biotechnologies, Madison, WI) overnight at 65ºC in 200 µL of

16 commercially provided reaction buffer (50 µM of ATP, 2.5 mM of $MnCl_2$). The resultant

17 solution was incubated at 80ºC for 10 min to inactivate the CircLigase, and then

18 gradually cooled down to 4ºC. To remove the non-circularized linear ssDNA template,

19 300U of Exonuclease I and 3,000 U of Exonuclease III (New England Biolabs, Beverly,

20 MA) were added to the solution. This solution was incubated at 37ºC for 3 h and was

21 then incubated at 80ºC for 40 min followed by gradual cooling down to inactivate the

22 exonucleases.

23 ### Hybridization of circular templates with Primer-1

24 The hybridization was carried out at room temperature for 2 hours by incubating

25 an equimolar solution of Primer-1 and circular DNA in TE buffer (pH 8.0, 10mM Tris,

26 1mM EDTA).

Synthesis of DNA meta-hydrogel by DNA polymerization

Circular DNA templates (50nM), which were hybridized with Primer-1, were incubated with Φ29 DNA polymerase (1 unit/μl) at 30°C for 4h in the reaction buffer (50mM Tris-HCl, 10mM $(NH_4)_2SO_4$, 10mM $MgCl_2$, 4mM dithiothreitol, 200μg/ml bovin serum albumin, 50mM dNTP). For MCA, Primer-2 and Primer-3 (50 pM of each) were then added into the resultant product to be incubated for 16 h at 30 °C without adding additional reagents.

Scanning Electron Microscope (SEM) imaging

Zeiss Ultra SEM (Carl Zeiss Inc., Germany) was used to obtain high resolution digital images of the DNA hydrogel. The DNA hydrogel was placed onto the top of the SEM holder. The sample was metal-coated with Au/Pd.

Focused-Ion Beam

FEI Strata 400 STEM FIB (FEI Company, USA) was used to cut individual DNA bird nest. The DNA bird nest was isolated from the DNA hydrogel and placed onto the top of SEM holder. The sample was metal-coated with Au/Pd.

Rheology Test

A Rheometric Scientific Inc. (RSI) rheometer with parallel cone and plate fixtures was used to measure the mechanical properties of the DNA hydrogel. A dynamic frequency sweeping mode was used, with the stain fixed at 50%.

Electrical Property Measurement

To test the ability of DNA meta-hydrogel as an electric circuit switch, gel was first formed in a mold that was similar to the "OFF" shape in Figure 5. Gold nanoparticles of 10 nm were doped into the gel during the gelation. The current vs voltage curves were measured using a Keithley 6430 (Keithley Instruments, Inc., USA).

Supporting figures

1   **Gel electrophoresis**

2   Linear ssDNA before circularization and circular template DNA were run in 10%

3   denature PAGE gel at 600 V at 25 °C for 1h with Tris-borate-EDTA (TBE, pH 8.3). The

4   gel was stained using the gel stain SYBR II (Molecular Probes, USA) following the

5   manufacturer's protocol.
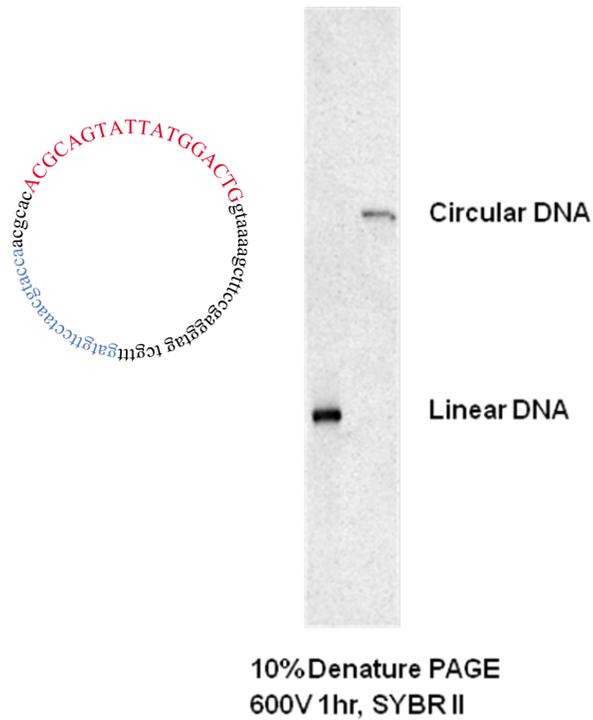
6

7   **Figure S1.** Gel electrophoresis image of circular DNA template. Lane 2 indicates circular

8   template DNA which shows slower mobility than linear DNA (Lane 1) after

9   circularization.

10 **Gel formation process monitoring**

11   The mixture for DNA polymerization was prepared first in a 96-well microliter

12 plate except Φ29 DNA polymerase. After Φ29 DNA polymerase was added, optical

13 density (OD) at 600 nm was evaluated by a microplate reader (BioTek Synergy4 Plate

14 Reader, BioTek Instruments, Inc., Winooski, Vermont) every hour at 30°C.

3

1
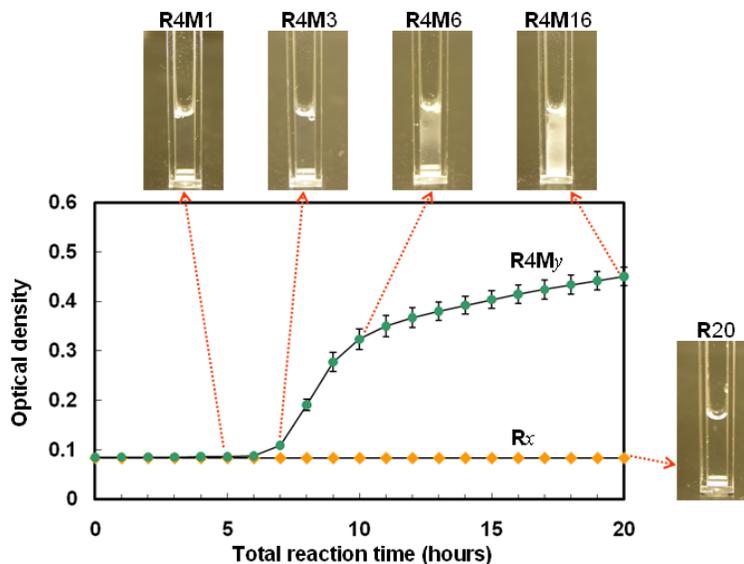
Figure S2. Monitoring the gel formation by optical density. OD of only RCA up to 20 h without MCA ($\bullet$, R_x) and 4 h RCA with MCA up to 16 h ($\bullet$, R_4M_y) were measured at a wavelength of 600 nm. Photographs of the cuvette containing R_4M_1, R_4M_3, R_4M_6, and R_4M_{16} showed clear visual changes of the gel going from transparent to opaque. However, R_x remained transparent up to 20 h.

Denaturing curve of the DNA hydrogel

The hydrogel was soaked in 50mM NaCl solution and the temperature was increased from 23 ^{o}C to 99 ^{o}C at a rate of 2 ^{o}C/min. The absorbance of the supernatant at 260 nm was recorded to obtain the denaturing curve. The denaturing temperature was determined as the temperature at which half of the gel was dissolved into the solution.
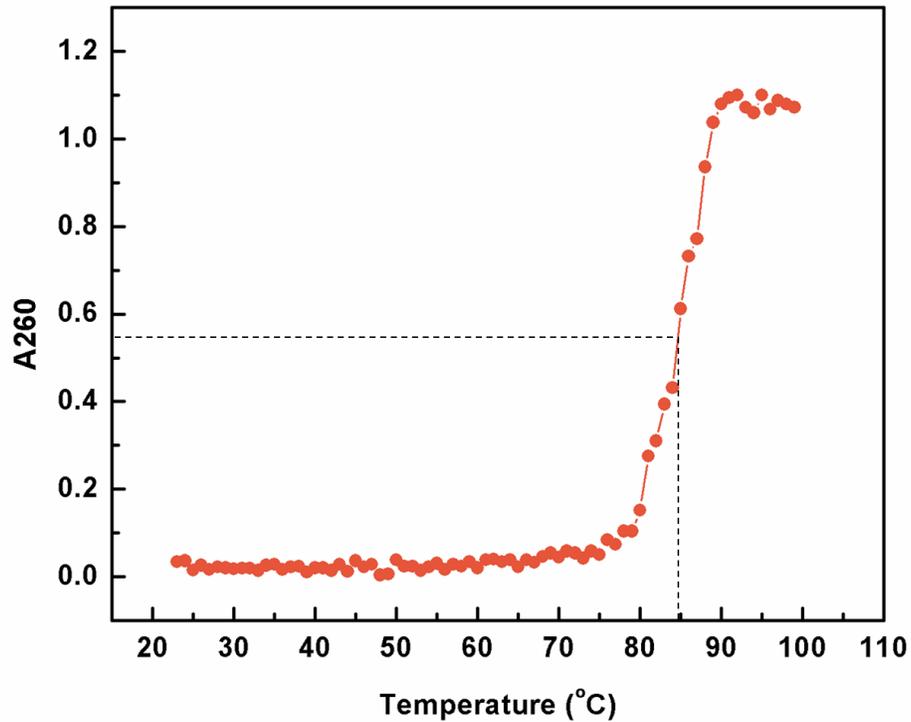
1

2   **Figure S3.** Denaturing curve of the DNA meta-hydrogel in 50mM NaCl.

3   **Remolding of the DNA hydrogel**
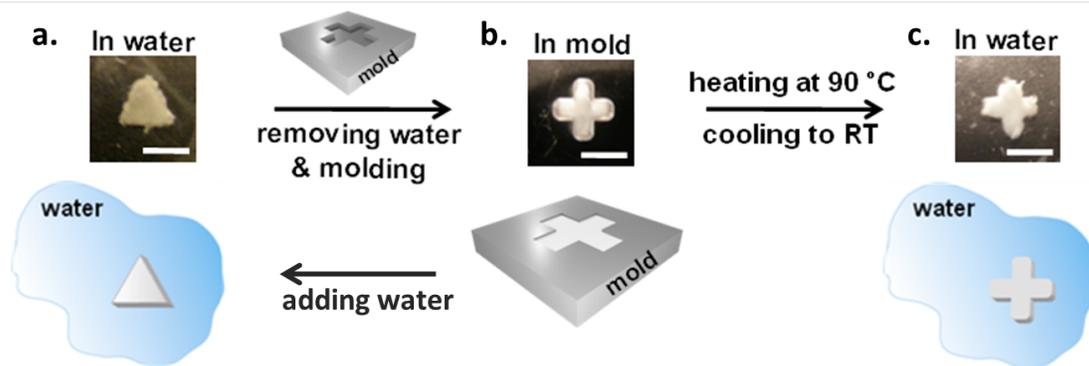
4

5   **Figure S4**: DNA hydrogel can be molded into new shape by heating processes. First,

6   triangle-shaped DNA hydrogel (**a**) was transferred to a cross-shaped mold (**b**) after

7   removing water. Then, by heating and cooling the gel to room temperature, the gel gain

8   new shape of the mold, cross-shape in water (**c**). All scale bars are 10 mm.
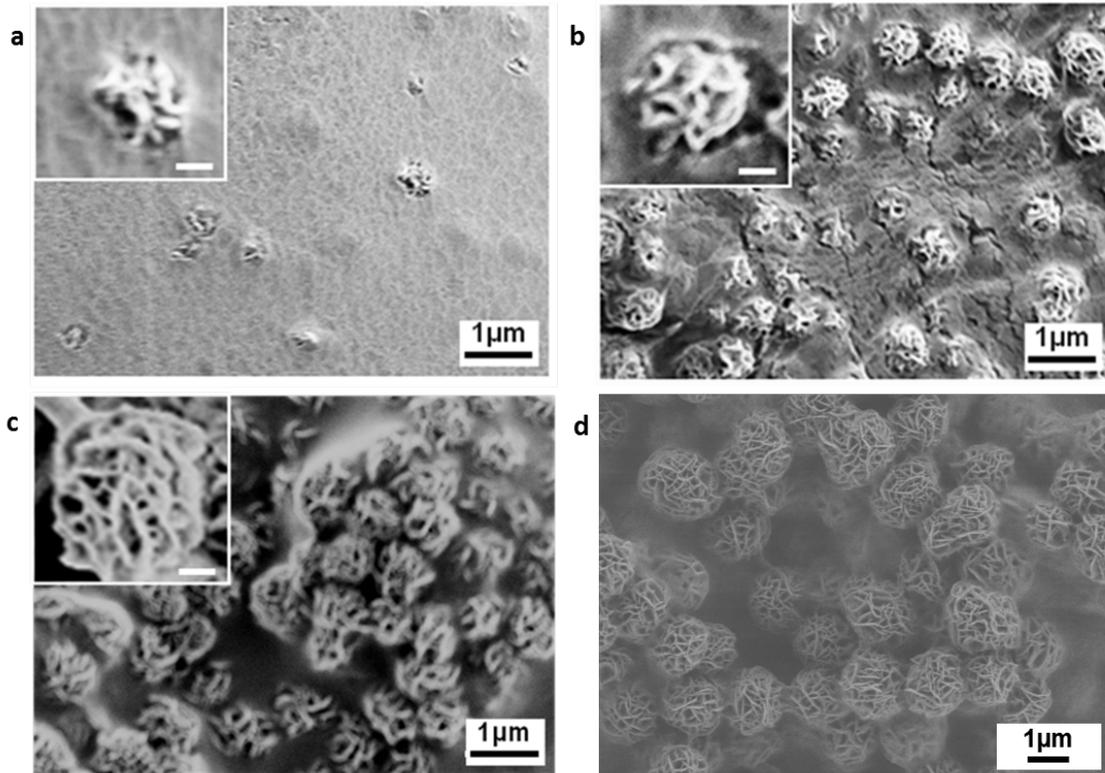
Figure S5: SEM image for different MCA time. **a**, R_4M_1, **b**, R_4M_3, **c**, R_4M_6, **d**, R_4M_{16}. Scale bars in insets, 200nm. Not only the number of the DNA bird nest were increasing, but also the diameters of DNA bird nests were growing from 350 ± 80nm for R_4M_1, 550 ± 100nm for R_4M_3, 790 ± 150nm for R_4M_6 and 1600 ± 200nm for R_4M_{16}.

Mechanical test of different DNA hydrogels

DNA hydrogels with different RCA time was produced (i.e. R_2M_{16}, R_4M_{16} and R_8M_{16}). Their mechanical properties were tested using the rheometer with the dynamic frequency sweeping mode at the fixed strain of 50%.
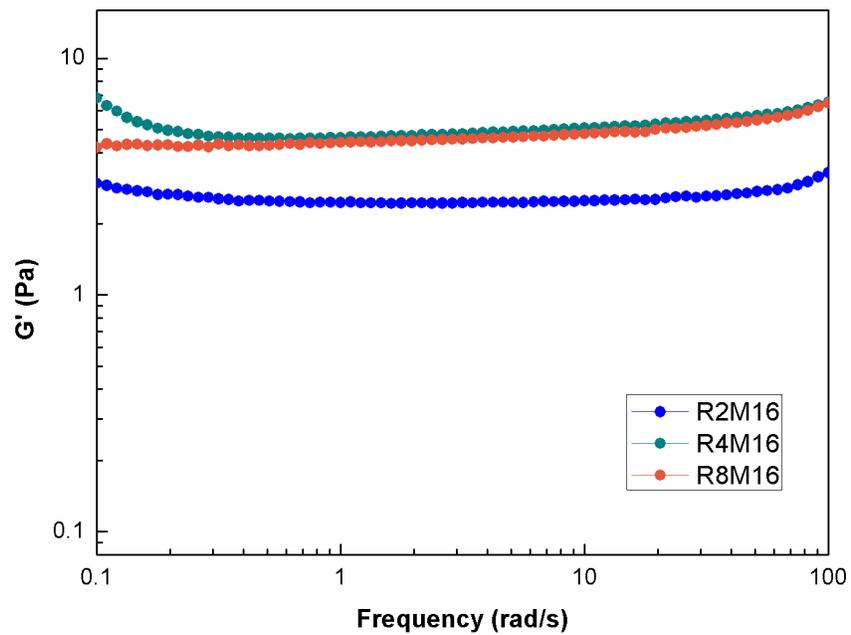
1

2   **Figure S6. Mechanical test of DNA hydrogel.** The shear storage modulus of the

3   hydrogels was between 2-10 Pa.

4   **Illustration for the mechanism of the liquid-like and solid-like properties**
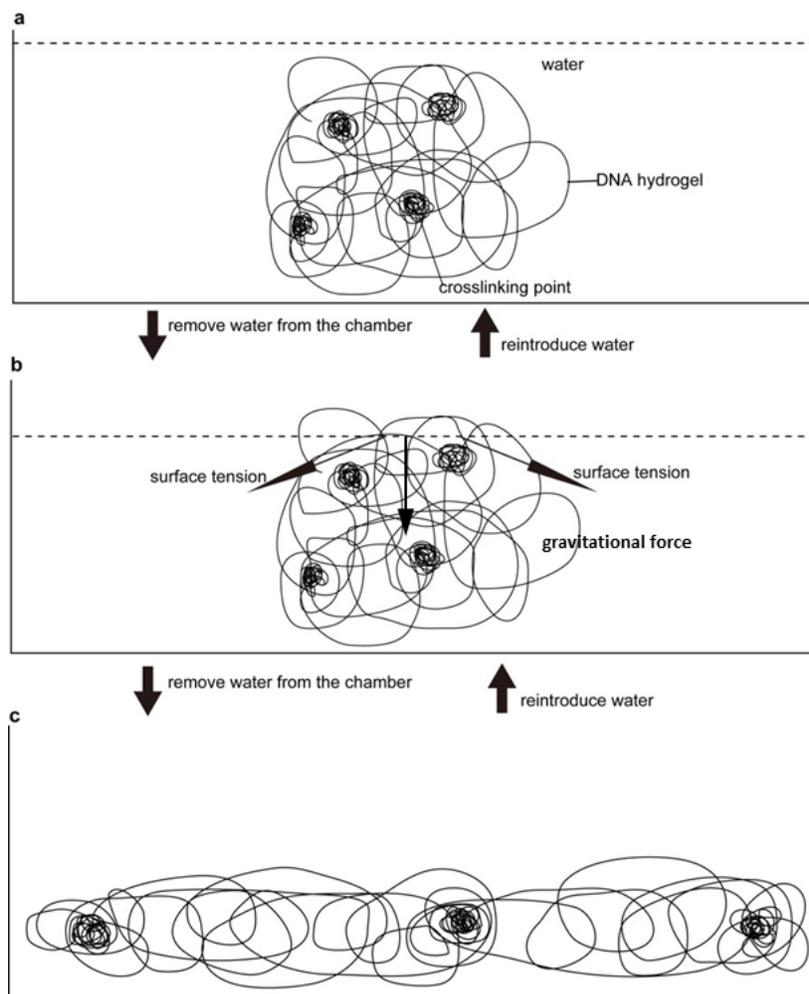
1

2 **Figure S7. Schematic molecular mechanism of the liquid-like property of the DNA**

3 **meta-hydrogel. a**, The DNA meta-hydrogel was a three-dimensional network composed

4 of DNA chains (both ssDNA and dsDNA) and the entangled crosslinking points. This

5 specific molecular structure endowed the hydrogel with very low modulus (~10 Pa).

6 When the hydrogel was in water, it exhibited solid-like property. **b,** After water was

7 removed from the chamber, the hydrogel was exposed to air. Because the hydrogel was

8 extremely soft, it could not keep its shape under the surface tension and gravitational

9 force, thus it was deformed at the water/air interface. **c**, After all the water was totally

10 removed from the chamber, under the action of surface tension and gravity, the gel

11 conformed to the shape of the chamber, resembling the property of water. After

12 reintroducing water into the chamber, the hydrogel returned to its birth shape, exhibiting

13 the solid-like property.

1   **Drug loading and in vitro drug release measurements**

2   We explored our hydrogel's potential as a controlled drug release system. A
3   unique advantage is that both the gel material building blocks (DNA) and the gel itself
4   (physical enclosure) can be used as drug reservoirs. We loaded our DNA hydrogel with
5   drugs, DOX and insulin, by intercalation and entrapment, respectively. As expected, the
6   drug release was sustained and significantly different depending on the loaded drugs.

7   To load drugs, green fluorescence dye labeled insulin solution (250 ng/μl, Sigma-
8   aldrich, St. Louis, MO) was added during gelling process (after three hour reaction) and
9   a doxorubicin (DOX) solution (20 ng/μl, Sigma-aldrich, St. Louis, MO), which
10   intercalates DNA, was incubated with DNA hydrogel in 1ml of distilled water for 48 h at
11   room temperature under gentle shaking. The water was refreshed after 48 h to remove
12   the unloaded drug. A fluorecence intensity of supernatant was measured to determine the
13   amount of unloaded drug. The entrapment efficiency (EE) was calculated based on
14   Equation (1):

15   EE (wt. %) = (1 - mass of unloaded drugs / mass of drug fed initially) × 100 %   (1)

16   Based on the equation, the EEs of DOX and Insulin were 60.0 % and 20.7 %,
17   respectively. After removing unloaded drug, the DNA hydrogel was directly immersed
18   into 500 μl of aqueous solution at a predetermined temperature (37°C). The amount of
19   DOX or Insulin released from the DNA hydrogel was measured by fluorecence intensity
20   (Doxorubicin at 590 nm and Insulin 512 nm). The cumulative drug release was calculated
21   using Equation (2):

22   Accumulated Drug Release [%] = $(M_t/M_o) \times 100$ (2)

23   Where M_t is the amount of accumulated drug released from the DNA hydrogel at time t,
24   and M_0 is the amount of drug loaded into the hydrogel. Here, M_0 was calculated by
25   subtracting the amount of unloaded drug from the drug fed.
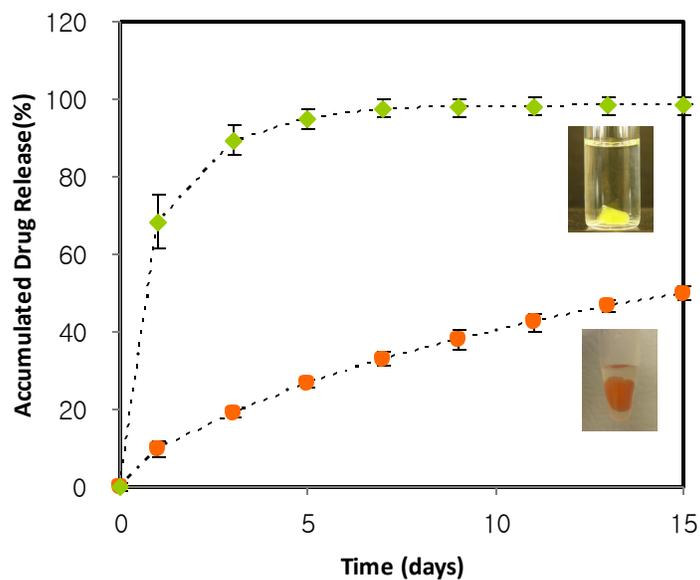
1

2 **Figure S8. Drug release profiles of R_4M_{16} DNA hydrogel.** Controlled drug release

3 profiles with insulin (♦) and doxorubicin (●). The volume of the DNA hydrogel was 70μl.

4 **Supporting tables**

5 **Table S1.** Oligonucleotide sequences of linear ssDNA and primers for the DNA hydrogel.

Strand	Sequence
Linear ssDNA	5'-Phosphate-**TCGTTTGATGTTCCTAACGTACCAACGCACACGCAGTATTATGGACTGGTAAAAGCTTTCCGAGGTAGCCTGGAGCATAGAGGCATTGGCTG**-3'
Primer1	5'-**TAGGAACATCAAACGACAGCCA**-3'(complementary to **TGGCTGTCGTTTGATGTTCCTA** in circular template)
Primer2	5'-**ACGCAGTATTATGGACTG**-3'
Primer3	5'-**TGGTACGTTAGGAACATC**-3'(complementary to **GATGTTCCTAACGTACCA** in circular template)

6

1 **Table S2.** Solid-like property and liquid-like property of DNA hydrogel depending on

2 reaction time **(R_xM_y)**.

Gel type (R_xM_y)	Solid-like property	Liquid-like property
R_0M_{16}*	NO	YES
R_1M_{16}*	NO	YES
R_2M_{16}	YES	YES
R_4M_{16}	YES	YES
R_8M_{16}	YES	YES
$R_{12}M_{16}$*	NO	YES
$R_{16}M_{16}$*	NO	YES
R_4M_1	NO	YES
R_4M_3	NO	YES
R_4M_6	NO	YES
R_4M_{20}	YES	YES
R_4M_{24}	YES	YES

3 ***:** These reactions resulted in turbid solutions with liquid-like properties (e.g. "flow").

4 However when they were transferred back into water, they did not maintain their original

5 shapes. Thus we defined them not having solid-like property.

6 ## Supporting Discussion

7 ### I. Discussion of the gel formation process

8   In detail, Primer-1 is hybridized with a circular DNA. The extremely long

9 ssDNA-1 is produced with a periodic sequence which is complementary of circular DNA

11

1 template via RCA. Primer-2 and Primer-3 are then added to reinforce the gel structure

2 without the need for additional Φ29 DNA polymerase. Since Primer-2 is complementary

3 to the portion of ssDNA-1, a number of Primer-2 are periodically hybridized to the

4 ssDNA-1, which is used as a template to become double-stranded DNA. During this

5 process, old strands, which are previously produced on same ssDNA-1, are displaced by

6 the advancing new strand. By this strong strand-displacement activity of Φ29 DNA

7 polymerase, the displaced strands become a new template, ssDNA-2, which is

8 complementary to primer-3. The displacement proceeds until the template perfectly

9 became double stranded DNA by the only a single Primer-2, which is hybridized at the

10 closest place to 5' end of ssDNA-1. In the similar fashion, the resulting ssDNA-2 is

11 hybridized with a number of Primer-3 to produce ssDNA-3, which is used to generate

12 new ssDNA-2 to enable to perform chain reaction.

13   Note that during each round of MCA, the ssDNA products could not exceed the

14 length of templates; in fact they became shorter in length due to the hybridization

15 position of primer-template not being at the end of the template. ssDNA-1 became double

16 stranded DNA at the end of Primer-2 elongation; thus ssDNA 1 could not server further

17 as templates. On the other hand, ssDNA-2 and ssDNA-3 were continuously produced;

18 the only limiting factors were the fact that they became shorter in length after each round.

19   Since the RCA and MCA products were very long (greater than 46 milliion Da,

20 Ref 1), and since the produced ssDNA-1 was complementary to ssDNA-2, these long and

21 linear DNA chains would entangle together as well as hybridize to each other at multiple

22 points, resulting in entangling the whole system into a gel-state.

23 **II. Discussion and calculation of the liquid-like and solid-like properties.**

24   There are three forces involved in deforming (or restoring) the gel when the water

25 was removed. They are elastic force εE, surface tension force γ/L and gravitational force

26 $\rho g L$. Here, ε is magnitude of the strain deformation, E is the Young's modulus, L is the

27 length scale of the gel, γ is the surface tension, ρ is the specific gravity of the gel and g is

28 the gravitational constant. For a DNA meta-hydrogel with the length scale of 1cm, the

1 elastic restoring force is $\varepsilon E = 5N/m^2$ for 100% strain deformation. The surface tension is

2 $7.2 N/m^2$ and the gravitational force is 98 N/m^2. Here we use $E = 5$ Pa, $\gamma = 0.072$ N/m,

3 $\rho = 1000$ kg/m^3 and $g = 9.8$ m/s^2. When the gel is taken out of water as shown in Figure

4 3c-f, both surface tension and gravitational force are sufficiently large to overcome the

5 elastic force and flatten the gel, which leads to liquid-like behavior. However, when the

6 gel is surrounded by water, both surface tension and gravity disappear, and the gel

7 restores to its original shape via elastic force.

8

9 **References:**

10 1   Blanco, L. *et al.*, Highly Efficient DNA-Synthesis by the Phage Phi-29 DNA-
11   Polymerase - Symmetrical Mode of DNA-Replication. *J. Biol. Chem.* **264,** 8935-
12   8940 (1989).
13
14